Enantiospecific Adsorption of (R)-3-Methylcyclohexanone on Naturally Chiral Cu(531)$^{R\&S}$ Surfaces

Ye Huang · Andrew J. Gellman

Abstract The enantiospecific adsorption and desorption of (R)-3-methylcyclohexanone on naturally chiral Cu(531)$^{R\&S}$ surfaces was studied using temperature programmed desorption. The Cu(531)$^{R\&S}$ surfaces are of interest because they lie at the center of the stereographic triangle and thus, have the highest density of chiral adsorption sites possible on the surface of a face centered cubic metal. Several (R)-3-methylcyclohexanone desorption features were resolved in the TPD spectra from Cu(531)$^{R\&S}$ surfaces and were assigned to desorption of molecules from terrace, step, and kink sites. The peaks associated with (R)-3-methylcyclohexanone desorbing from the R- and S-kink sites differed in temperature by 2.2 ± 0.6 K. This corresponds to an enantiospecific difference in the desorption energies of 0.5 ± 0.2 kJ/mol, with a preference for adsorption of (R)-3-methylcyclohexanone at the S-kinks on the Cu(531)^{S} surface.

Keywords Chiral · Enantioselective · Enantiospecific · Surface · High Miller index · Copper

1 Introduction

Many organic molecules are chiral and thus, exist in two forms that are non-superimposable mirror images of one another. The two non-superimposable forms of chiral molecules, called enantiomers, have identical physical and chemical properties in achiral environments. Because life on Earth is based on proteins and enzymes that are homochiral, living organisms are chiral environments. As a result, the two enantiomers of a chiral compound behave differently when ingested by living organisms. Thus, in order to achieve the desired therapeutic effects, chiral pharmaceuticals must be produced in enantiomerically pure form. This raises great interest in the development and use of chiral media for enantiospecific production of enantiomerically pure pharmaceuticals [1].

Currently, the most common method used to produce an enantiomerically pure compound is to prepare a racemic mixture of its two enantiomers by traditional synthesis using achiral reactants, followed by separation of the racemic mixture into its enantiomerically pure components. Methods such as selective crystallization [2] and chiral chromatography [3] can be used to separate the racemic mixture. The drawback of synthesizing a racemic mixture and then separating the two enantiomers is that it wastes starting materials and the separation process is always expensive. Hence, the production of enantiomerically pure products via a direct enantioselective catalytic route is very attractive, provided that one can identify and prepare appropriate chiral catalysts.

The most common strategy for preparation of a chiral catalytic surface is via the adsorption of chiral organic modifiers that impart chirality to an achiral surface [4, 5]. Examples of successful enantioselective catalysts based on this methodology include the tartaric acid modified Ni-based catalysts [6] and cinchona alkaloid modified Pt-based catalysts [7]. Alternatively, one can use a crystalline solid with an achiral bulk lattice but expose a high Miller index chiral surface with a structure that lacks mirror plane symmetry. Any surface of a face center cubic material will be chiral

Y. Huang
Department of Chemical Engineering, Carnegie Mellon University, Pittsburgh, PA 15213, USA

A. J. Gellman (✉)
National Energy Technology Laboratory, U.S. Department of Energy, P.O. Box 10940, Pittsburgh, PA 15236, USA
e-mail: gellman@cmu.edu

provided that its Miller indices, (hkl), satisfy the constraints $h \neq k \neq l \neq h$ and $h \cdot k \cdot l \neq 0$ [8]. The first such surface that was shown to be naturally chiral was Ag(643)$^{R\&S}$ and the most thoroughly studied, naturally chiral surface is Cu(643)$^{R\&S}$ [8–17]. These high Miller index chiral surfaces expose complex surface structures which are often described as being composed of terrace, step, and kink microfacets [18]. The chiral kink sites on these surfaces have the potential to interact enantiospecifically with chiral molecules. It has been shown that chiral molecules such as (R)-3-methylcyclohexanone will adsorb enantiospecifically on the chiral kink sites of the Cu(643)$^{R\&S}$ surfaces [10].

The ideal structures of most high Miller index surfaces of face centered cubic metals can be thought of as being formed of low Miller index microfacets that form terraces, steps, and kinks [18]. This simple notion has been extremely useful in interpreting the properties of such surfaces, although a more sophisticated classification system has been proposed recently that classifies surfaces based on their symmetry properties and on the exposure of specific atomic structures [19]. The concept of the terrace-step-kink structure of a surface clearly breaks down for the Cu(531)$^{R\&S}$ surfaces used in this work and shown in Fig. 1. These surfaces lie at the center of the stereographic projection. As such, the three low Miller index microfacets which they expose are all one lattice spacing in width and one cannot legitimately denote them as terrace, step, or kink. In some sense, this surface can be considered to expose only kink sites and to expose the highest density of chiral kinks possible among the surfaces of face centered cubic metals.

One complicating factor in considering enantioselective adsorption on the naturally chiral high Miller index faces of metals is that their real surfaces structures are not those of the ideal termination of the bulk crystal. Diffusion of atoms along step edges leads to thermal roughening. On the Cu(643) surfaces this leads to the coalescence of kinks and lengthening of the straight step edges. This has been modeled using molecular simulation methods and recently

confirmed by STM images of the surface [20–22]. Although, no comparable studies have been performed of the Cu(531) surface it must be subject to the same roughening phenomena. Structural studies of the Pt(531) surface have been attempted using low-energy electron diffraction (LEED) and DFT [23, 24]. Although those studies could not have revealed roughening in the way that STM imaging does, they do provide evidence of large relaxations of the topmost layers of the surface and evidence of the displacement of atoms from the topmost layer into an adlayer. Thus, the true structure of the Cu(531) surface is probably more complex than those of the ideal terminations shown in Fig. 1. The true structures probably expose low Miller index microfacets and step edges with a range of different widths. Nonetheless, observations of the enantioselectivity of (R)-2-bromobutane decomposition and the enantiospecificity of the orientations of (R)- and (S)-alanine adsorbed on Cu(531)$^{R\&S}$ surfaces indicates that they remain chiral in spite of surface roughening [11, 25].

The work reported here probes the enantioselective adsorption of (R)-3-methylcyclo-hexanone on the Cu(531)$^{R\&S}$ surfaces and compares it to adsorption on the well studied Cu(643)$^{R\&S}$ surfaces [10]. The results reveal enantiospecific adsorption on the Cu(531)$^{R\&S}$ surfaces but no indication that they are more enantioselective than the Cu(643)$^{R\&S}$ surfaces.

2 Experimental

All experiments were conducted in a stainless steel ultra-high vacuum (UHV) chamber with a base pressure of 2×10^{-10} Torr. The UHV chamber was equipped with an Ar$^+$ ion sputtering gun to clean the surface, LEED optics to determine surface structure, a quadrupole mass spectrometer (QMS) to perform temperature programmed desorption (TPD), and an X-ray source and electron energy analyzer for X-ray photoemission spectroscopy (XPS).

Cu(531)^R **Cu(531)^S**

Fig. 1 Models of the ideally terminated Cu(531)$^{R\&S}$ surfaces. The unit cell is superimposed on the figure, as are the three low Miller index microfacets that intersect to form the surface structure. In this figure, the different shading of the atoms indicates their different coordination numbers. For example, the darkest atoms have a coordination number of 6. The less dark atoms have a coordination number of 8 and the lightest atoms have a coordination number of 9
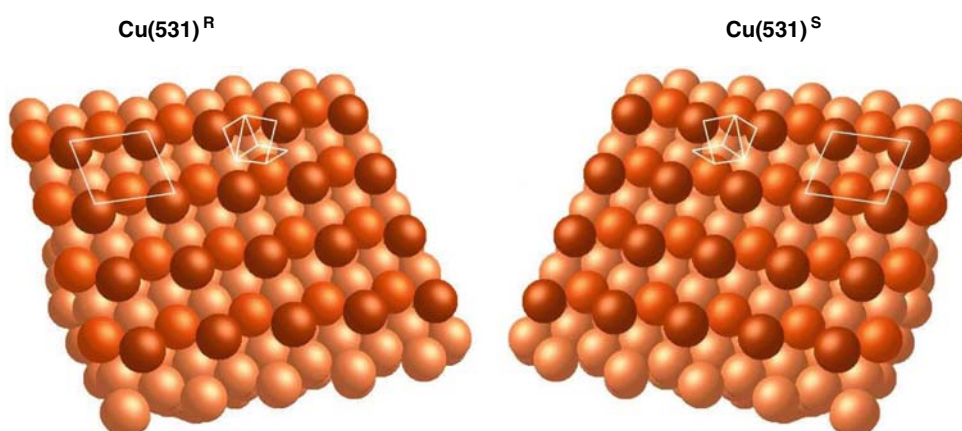
The Cu(531) single crystal (99.99% purity) was obtained from Monocrystal Company. The crystal was 10 mm in diameter and 2 mm thick. The crystal was mounted between two tantalum wires spot-welded to its edges. The two tantalum wires were attached to a sample holder at the bottom of a UHV manipulator. The crystal could be cooled down to ~80 K and can be heated resistively to over 1,000 K with the temperature measurement made by using a chromel-alumel thermocouple spot-welded to the edge of the crystal.

The crystal was cleaned by cycles of Ar^+ ion sputtering (1.5 keV, 20 μA) and annealing to 1,000 K. Both sides of the crystal were cleaned using identical procedures. It was necessary to clean both sides of the Cu(531) single crystal because the two opposite faces are enantiomers and both were used. The surface structures of crystals were verified by LEED. The handedness of the chiral surfaces were determined by x-ray diffraction (XRD) as described elsewhere [11].

(R)-3-Methylcyclohexanone (98%) was purchased from Aldrich Chemical Co. It was transferred to a glass vials and subjected to several cycles of freezing, pumping, and thawing to remove impurities before exposing onto the surface through a standard leak valve. The purity of the sample was verified by mass spectrometry. Exposures were reported in units of Langmuirs (L) and were not corrected for ion gauge sensitivities to different gas species.

Temperature programmed desorption (TPD) experiments were performed by first cooling the Cu sample with liquid nitrogen to ~80 K. (R)-3-Methylcyclohexanone was then adsorbed by exposure of the sample to the vapor from a doser with the Cu sample held at 80 K. Desorption measurements were performed by heating the Cu sample at a constant rate (1 K/s) and while using the QMS to monitor the species desorbing from the surface. XPS analysis showed that (R)-3-methylcyclohexanone adsorption and desorption contaminated the surface with small amounts of carbon after each TPD experiment so; the surfaces were cleaned by Ar^+ sputtering and annealing prior to each TPD experiment.

3 Results

3.1 Coverage-Dependent Adsorption of (R)-3-Methylcyclohexanone on Cu(531)

In order to probe the different adsorption sites occupied by (R)-3-methylcyclohexanone on the Cu(531)^S surface, TPD spectra were obtained after adsorption at various different initial coverages. The TPD spectra shown in Fig. 2 reveal four significant features which appear sequentially with increasing exposure. At low coverages a peak first appears
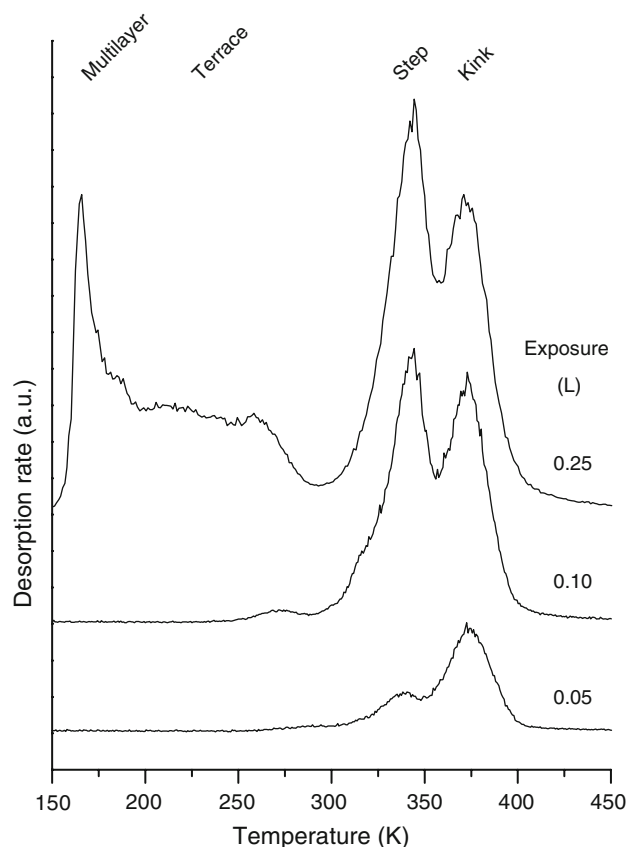
Fig. 2 TPD spectra of (R)-3-methylcyclohexanone on the Cu(531)^S surface. The data shown was obtained by monitoring the signal at $m/q = 69$ using the QMS. The exposure is in units of Langmuir (1 L = 1.0×10^{-6} Torr s). The highest temperature desorption peak at ~375 K is assigned to the desorption of (R)-3-methylcyclohexanone from the kink sites of Cu(531)^S. The desorption peak at ~345 K is assigned to the desorption of (R)-3-methylcyclohexanone from step sites and the broad feature from 200–270 K is assigned to the desorption of (R)-3-methylcyclohexanone from terrace sites of Cu(531)^S. The low temperature peak at ~165 K is assigned to desorption of the (R)-3-methylcyclohexanone multilayer

at 375 K followed by another at 345 K. By analogy with the TPD spectra obtained previously for (R)-3-methylcyclohexanone desorption from the Cu(643)$^{R\&S}$ surfaces and other Cu surfaces vicinal to the (111) plane [10], we can assign the peaks at 375 K and then 345 K to the desorption of (R)-3-methylcyclohexanone molecules from kink and step sites, respectively, on Cu(531)^S. As the exposure to (R)-3-methylcyclohexanone increased, the desorption peak from the kink sites saturated first, followed by the saturation of the desorption feature from the step sites. The TPD spectra in Fig. 2 show that as the (R)-3-methylcyclohexanone coverage increases further, a broad desorption feature appears in the temperature range 200–270 K. Again, by analogy with the results obtained from the Cu(111) surface [10], this was assigned to the desorption of molecules from terrace sites on Cu(531)^S. The sequential filling of the kink,

step and terrace sites indicate that the adsorption energy of
(R)-3-methylcyclohexanone at various sites decreases
sequentially in the order kink, step and terrace. Finally, at
the highest coverages, a very sharp desorption peak appears
at 165 K. In agreement with previous studies this corre-
sponds to the formation of (R)-3-methylcyclohexanone
multilayers on the Cu(531)^S surface [10].

3.2 Enantiospecific Adsorption of (R)-3-Methylcyclohexanone on Cu(531)$^{R\&S}$

Enantiospecific adsorption was studied by comparing the
TPD spectra of (R)-3-methylcyclohexanone monolayers on
both Cu(531)^R and Cu(531)^S surfaces. To ensure the satu-
ration of the (R)-3-methylcyclohexanone monolayer, the
exposure used was 0.3 L and the substrate was kept at
200 K during exposure. As is apparent from the TPD
spectra in Fig. 2, these conditions are sufficient to saturate
the monolayer, but the adsorption temperature is high
enough that there is no multilayer adsorption. Five TPD
spectra were acquired using monolayer coverages of (R)-3-
methylcyclohexanone on both the Cu(531)^R and the
Cu(531)^S surfaces. The TPD spectra from Cu(531)^R and
Cu(531)^S surface are compared in Fig. 3. Similar desorp-
tion features from terrace, step and kink sites appear on
both Cu(531)^R and Cu(531)^S surfaces. The inset to Fig. 3
highlights the features associated with the desorption of
(R)-3-methylcyclo-hexanone from the chiral kink sites on
the Cu(531)^R and Cu(531)^S surfaces. These demonstrate
the fact that (R)-3-methylcyclohexanone binds more
strongly to the kinks on the Cu(531)^S surface than those on
the Cu(531)^R surface. In order to most accurately estimate
the peak temperatures, all ten such TPD peaks obtained
from the 10 independent TPD experiments have been fit
with Gaussian functions. The peak desorption rates of (R)-
3-methylcyclohexanone from chiral kink sites occur at
$T_p = 372.7 \pm 0.4$ K on Cu(531)^S and $T_p = 370.5 \pm 0.4$ K
on Cu(531)^R. The difference in peak desorption tempera-
tures of $\Delta T_p = 2.2 \pm 0.6$ K corresponds to a difference in
desorption energies of $\Delta\Delta E_{des} = 0.5 \pm 0.2$ kJ/mol, as
estimated using the Redhead equation for first-order
desorption with a pre-exponential factor of 10^{13} s^{-1}. This
is a direct manifestation of the enantiospecific interaction
of (R)-3-methylcyclohexanone molecules with the natu-
rally chiral kink sites on the Cu(531)^R and Cu(531)^S
surfaces.

4 Discussion

The results presented in Figs. 2 and 3 reveal two interesting
features of the adsorption of (R)-3-methylcyclohexanone
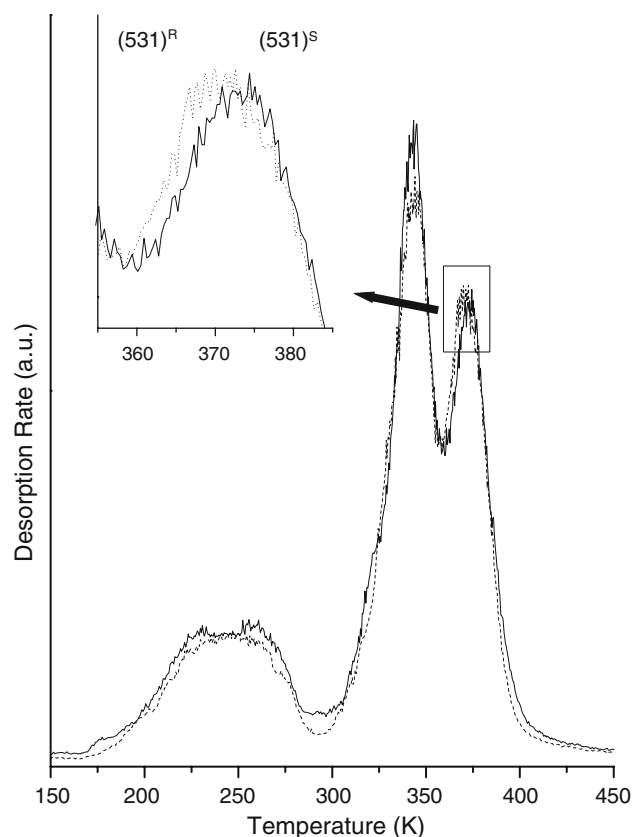
Fig. 3 TPD spectra of (R)-3-methylcyclohexanone on the
Cu(531)$^{R\&S}$ surfaces. The data shown was obtained by monitoring
the signal at $m/q = 69$ using the QMS. Both exposures are 0.30 L
(1 L $= 1.0 \times 10^{-6}$ Torr s) but with the surface held at 200 K. The
three desorption features from terrace, step and kink sites appear in
the spectra from both Cu(531)^R and Cu(531)^S surfaces. The inset
shows the difference of desorption peak temperature of (R)-3-
methylcyclohexanone on the R- and S-chiral kink sites of Cu(531)$^{R\&S}$.
(R)-3-Methylcyclohexanone binds more strongly to the Cu(531)^S
surface than to the Cu(531)^R surface

on the Cu(531)$^{R\&S}$ surfaces; the types of adsorption sites
exposed by these surfaces and their enantioselectivity. The
TPD spectra in Fig. 2 illustrate that the adsorption of (R)-3-
methylcyclohexanone on Cu(531)$^{R\&S}$ surfaces is phenom-
enologically similar to that on the Cu(643)$^{R\&S}$ in the sense
that individual molecules can be considered to bind at
terrace, step or kink sites [10]. Integration of the area under
each of the three desorption features in the TPD spectrum
of a monolayer (R)-3-methylcyclohexanone desorption
gives an estimate of roughly 23% binding to terrace sites,
44% binding to step sites, and 33% binding to kink sites.
The sequence in which these sites are filled is consistent
with a model for adsorption in which the molecules find the
highest energy binding site first and occupy binding sites
with sequentially lower binding affinity as coverage is
increased. The previous assignment of well defined
adsorption sites to distinct desorption peaks has been made
by comparing (R)-3-methylcyclohexanone TPD spectra

from the following set of surfaces: Cu(111) (terrace only); Cu(221) and Cu(533) (formed of (111) terraces separated by straight step edges); and Cu(643) and Cu(653) (formed of (111) terraces separated by kinked step edges). What is very surprising, is the fact that one can describe (R)-3-methylcyclohexanone adsorption on the Cu(531)$^{R\&S}$ surfaces in these terms. The ideal structure of the Cu(531)$^{R\&S}$ surfaces cannot be described as having terrace, steps, and kink because each of the three low Miller index microfacets that form the surface is one atomic diameter in its lateral dimension. Furthermore, the ideal unit cell of a Cu(531) surface is 4.5 Å on a side which is significantly smaller than the molecular diameter of (R)-3-methylcyclohexanone which is 7.5 Å. The observation of the three well defined desorption features in the TPD spectra suggests that surface roughening results in the formation of terraces and straight step edges that are significantly wider than the single unit cell microfacets exposed by the ideal structure. Such thermal roughening has been predicted beforehand for the clean high Miller index surfaces [22] but may also be influenced by the adsorption of the (R)-3-methylcyclohexanone [12].

The enantiospecific interaction between (R)-3-methyl-cyclohexanone molecules and the chiral kink sites on the Cu(531)$^{R\&S}$ surfaces manifests itself in the TPD spectra of Fig. 3. (R)-3-Methylcyclohexanone was found have a higher adsorption energy at the kink sites of Cu(531)^{S} than at those on Cu(531)^{R}. The difference in the desorption energies from these two sites is estimated to be $\Delta\Delta E_{des} = 0.5 \pm 0.2$ kJ/mol. This can be compared with the results of similar experiments on the Cu(643)$^{R\&S}$ surfaces which revealed an enantiospecific desorption energy difference of $\Delta\Delta E_{des} = 1.0 \pm 0.2$ kJ/mol [10]. As in the case of the Cu(643)$^{R\&S}$ surfaces, the TPD feature associated with (R)-3-methylcyclohexanone molecules desorbing from the steps showed no enantiospecificity. The net result is that adsorption and desorption at kink sites on the naturally chiral surface of Cu is enantiospecific. On the Cu(643)$^{R\&S}$ surfaces the enantiospecific adsorption of (R)-3-methylcyclohexanone at the kinks is also manifested in the adsorption geometries as probed by infrared absorptions spectroscopy. Although the details of the adsorption geometry at the kinks is not known the overall orientation is one with the molecular ring lying flat against the surface and the >C=O bond providing the bulk of the interaction with the kink [26]. The interesting result of comparison of the (R)-3-methylcyclohexanone TPD spectra on the Cu(643)$^{R\&S}$ and the Cu(531)$^{R\&S}$ surfaces is that the Cu(531)$^{R\&S}$ surfaces do not appear to expose any more kinks than the Cu(643)$^{R\&S}$ surfaces, nor do the Cu(531)$^{R\&S}$ surfaces display any greater enantiospecificity than the Cu(643)$^{R\&S}$ surfaces.

5 Conclusions

The desorption of (R)-3-methylcyclohexanone from the Cu(531)$^{R\&S}$ surfaces and the Cu(643)$^{R\&S}$ surfaces has been shown to be quite similar in spite of distinct differences between their ideal surface structures. The Cu(643)$^{R\&S}$ surfaces have structures formed of well defined (111) terraces, (100) steps and (110) kinks. Temperature programmed desorption spectra of (R)-3-methylcyclohexanone from the Cu(643)$^{R\&S}$ surfaces reveal three well-resolved features at 230 K, 345 K, and 385 K that can be readily assigned to molecules desorbing from the (111) terraces, (100) steps, and (110) kinks, respectively. The Cu(531)$^{R\&S}$ surfaces have structures that are based on the same three low Miller index microfacets but they cannot be classified as terraces, steps, or kinks because all three microfacets are of the same size and are smaller than the dimensions of (R)-3-methylcyclohexanone. The surprising result of the work presented in this paper is that, nonetheless, the desorption of (R)-3-methylcyclohexanone from Cu(531)$^{R\&S}$ reveals the same three features as on Cu(643)$^{R\&S}$. Furthermore, the feature assigned to (R)-3-methylcyclohexanone desorbing from the chiral kinks on the Cu(531)$^{R\&S}$ exhibits enantiospecific differences in the desorption energies of $\Delta\Delta E_{des} = 0.5 \pm 0.2$ kJ/mol with the (R)-3-methylcyclohexanone bound more strongly to the S-kinks on the Cu(531)^{S} surface than the R-kinks on the Cu(531)^{R} surface. This is less than the enantiospecific adsorption energy difference on the Cu(643)$^{R\&S}$ surfaces. Thus, although the Cu(531)$^{R\&S}$ surfaces have the greatest density of chiral kinks possible on the surface of a face centered cubic metal, they are not the most enantiospecific for adsorption of (R)-3-methylcyclohexanone.

References

1. Mallat T, Orglmeister E, Baiker A (2007) Asymmetric catalysis at chiral metal surfaces. Chem Rev 107:4863–4890
2. McCague RAS (1999) Applications of crystallization technology in chiral synthesis. Innov Pharm Technol 99:100–104
3. Francotte E (1996) An essential and versatile tool in the research and in the development of bioactive compounds. Chim Nouv 14:1541
4. Lorenzo MO, Baddeley CJ, Muryn C, Raval R (2000) Extended surface chirality from supramolecular assemblies of adsorbed chiral molecules. Nature 404:376–378
5. Parschau M, Romer S, Ernst KH (2004) Induction of homochirality in achiral enantiomorphous monolayers. J Am Chem Soc 126(47):15398–15399
6. Izumi Y (1983) Modified raney-nickel (MRNI) catalyst—heterogeneous enantio-differentiating (asymmetric) catalyst. Adv Catal 32:215–271

7. Baiker A (1997) Progress in asymmetric heterogeneous catalysis: design of novel chirally modified platinum metal catalysts. J Mol Catal A-Chem 115(3):473–493

8. Sholl DS, Asthagiri A, Power TD (2001) Naturally chiral metal surfaces as enantiospecific adsorbents. J Phys Chem B 105(21):4771–4782

9. McFadden CF, Cremer PS, Gellman AJ (1996) Adsorption of chiral alcohols on ''chiral'' metal surfaces. Langmuir 12(10): 2483–2487

10. Horvath JD, Gellman AJ (2002) Enantiospecific desorption of chiral compounds from chiral Cu(643) and achiral Cu(111) surfaces. J Am Chem Soc 124(10):2384–2392

11. Rampulla DM, Francis AJ, Knight KS, Gellman AJ (2006) Enantioselective surface chemistry of R-2-bromobutane on Cu(643)$^{R\&S}$ and Cu(531)$^{R\&S}$. J Phys Chem B (submitted for publication)

12. Zhao XY, Perry SS, Horvath JD, Gellman AJ (2004) Adsorbate induced kink formation in straight step edges on Cu(533) and Cu(221). Surf Sci 563(1–3):217–224

13. Gellman AJ, Horvath JD, Buelow MT (2001) Chiral single crystal surface chemistry. J Mol Catal A-Chem 167(1–2):3–11

14. Horvath JD, Gellman AJ (2001) Enantiospecific desorption of R- and S-propylene oxide from a chiral Cu(643) surface. J Am Chem Soc 123(32):7953–7954

15. Zhao XY, Perry SS (2004) Ordered adsorption of ketones on Cu(643) revealed by scanning tunneling microscopy. J Mol Catal A (in press)

16. Kamakoti P, Horvath J, Gellman AJ, Sholl DS (2004) Titration of chiral kink sites on Cu(643) using iodine adsorption. Surf Sci 563(1–3):206–216

17. Rampulla DM, Gellman AJ (2006) Enantioselective decomposition of chiral alkyl bromides on Cu(643)$^{R\&S}$: effects of moving the chiral center. Surf Sci (to be submitted)

18. van Hove MA, Somorjai GA (1980) New microfacet notation for high-Miller-index surfaces of cubic materials with terrace, step, and kink structures. Surf Sci 92(2–3):489–518

19. Jenkins SJ, Pratt SJ (2007) Beyond the surface atlas: a roadmap and gazetteer for surface symmetry and structure. Surf Sci Rep 62(10):373–429

20. Baber AE, Gellman AJ, Sholl DS, Sykes ECH (2008) The real structure of naturally chiral Cu(643). J Phys Chem C (in press)

21. Asthagiri A, Feibelman PJ, Sholl DS (2002) Thermal fluctuations in the structure of naturally chiral Pt surfaces. Top Catal 18(3–4):193–200

22. Power TD, Asthagiri A, Sholl DS (2002) Atomically detailed models of the effect of thermal roughening on the enantiospecificity of naturally chiral platinum surfaces. Langmuir 18(9):3737–3748

23. Puisto SR, Held G, King DA (2005) Energy-dependent cancellation of diffraction spots due to surface roughening. Phys Rev Lett 95(3):036102

24. Puisto SR, Held G, Ranea V, Jenkins SJ, Mola EE, King AA (2005) The structure of the chiral Pt(531) surface: a combined LEED and DFT study. J Phys Chem B 109(47):22456–22462

25. Gladys MJ, Stevens AV, Scott NR, Jones G, Batchelor D, Held G (2007) Enantiospecific adsorption of alanine on the chiral Cu(531) surface. J Phys Chem C 111:8331–8336

26. Horvath JD, Baker L, Gellman AJ (2008) Enantiospecific orientation of R-3-Methylcyclohexanone on the chiral Cu(643)(R/S) surfaces. J Phys Chem C 112(20):7637–7643